

Article

Synthesis, Crystal Structure, Magnetic Property and Photo-Induced Coloration of a One-Dimensional Chain Complex

Qingguo Meng, Suqing Wang, Junhao Zhang, Rui Xun, Mingchao Chen and Jitao Lu *

College of Chemical Engineering and Environmental Chemistry, Weifang University, Weifang 261061, China; mengqg@wfu.edu.cn (Q.M.); wsuqing66@163.com (S.W.); 17865675166@163.com (J.Z.); 17865670125@163.com (R.X.); cmingchao16@163.com (M.C.)

* Correspondence: lujitao@foxmail.com

Academic Editor: Helmut Cölfen

Received: 1 January 2017; Accepted: 1 March 2017; Published: 8 March 2017

Abstract: A novel photoactive complex was constructed from two non-photoactive ligands and cobalt (II) ions. Upon ultra violet (UV) irradiation (365 nm), the color of complex **1** changes from orange to violet. The ESR spectrum indicates that the photoactive phenomenon of complex **1** originates from an intermolecular energy transfer between the H₅DDCPBA ligand and phenanthroline ligand. This photoactive complex shows high thermal stability according to the investigation of thermogravimetric analyses. In addition, the temperature dependence of magnetic susceptibilities for the orange complex **1** was also investigated systematically.

Keywords: photoactive complex; ESR spectrum; intermolecular energy transfer; magnetic properties; non-photoactive ligands

1. Introduction

In the past two decades, metal organic coordination polymers, as a class of complexes constructed by metal ions and organic bridging ligands through coordination bonds, have attracted great research interest due to their intriguing structural topologies and potential applications in catalysis, separation, electronics, luminescence, drug delivery and gas storage, etc. [1–11]. In all kinds of applications, photo properties of metal organic coordination polymers have attracted increasing attention, especially for their development of photoresponsive materials based on metal–ligand complexes, due to their value and importance to the development of advanced molecular electronic and photonic devices. For example, Fu and coworkers have reported a series of new types of photochromic molecular systems based on the viologen ligand [12–14]. Champness's group has reported a metal-bearing coordination network synthesized from Re(2,2'-bipyridine-5,5'-dicarboxylate)(CO)₃Cl bridging ligands and Cu(II) nodes, which undergoes an irreversible photoinduced charge transfer process [15]. Compared to the traditional pure organic and inorganic molecular systems, the photoresponsive materials based on metal–ligand complexes can be perturbed and tuned by the connection of different metal centers and photochromic ligands. It is worth pointing out that although quite a number of classes of metal complexes with different photochromic ligands have been developed in recent years, the photoresponsive frameworks constructed from non-photochromic ligands are still rare to the best of our knowledge. Only Fu reported a photoactive Zn(II) complex using two non-photoactive components [16].

In the present paper, one novel photoactive complex was constructed from two non-photoactive ligands and cobalt (II) ions, [Co(HDDCPBA)_{0.5}(Phen)(H₂O)₂] \cdot 2H₂O [**1**, H₅DDCPBA = 3,5-di(3'/5'-dicarboxyl-phenyl) benzoic acid, Phen = 1,10-phenanthroline]. Upon ultra violet (UV) irradiation

(365 nm), orange crystal of **1** becomes violet. The photoactive phenomenon of complex **1** originates from an inter-ligand energy transfer between the DDCPBA ligand and phenanthroline ligand. This work provides a new route to a prepared photoactive system from non-photochromic ligands.

2. Experimental

2.1. Materials and Methods

All chemicals were of reagent grade and were used as commercially obtained without further purification. Elemental analyses (for C, H or N) were carried out on a Perkin-Elmer 240 elemental analyzer. Powder X-ray diffraction measurements were performed with a Bruker AXS D8 Advance instrument (Karlsruhe, Germany). The Fourier Transform Infrared (FT-IR) spectra were recorded in the range 4000–400 cm^{-1} on a Nicolet 330 FTIR Spectrometer using the KBr pellet method. Thermogravimetric analysis (TGA) experiments were performed using a Perkin-Elmer TGA 7 instrument (PerkinElmer, Billerica, MA, USA) (heating rate of 10 $^{\circ}\text{C min}^{-1}$, nitrogen stream). Electronic absorption spectra were recorded on a Hitachi U-4100 spectrophotometer. The ESR spectrum was recorded on a JEOL JES-FA200 (JEOL, Tokyo, Japan).

2.2. Synthesis of $[\text{Co}(\text{HDDCPBA})_{0.5}(\text{Phen})(\text{H}_2\text{O})_2] \cdot 2\text{H}_2\text{O}$ (**1**)

Heating a mixture of H_5DDCPBA (2.0 mg, 0.004 mmol), $\text{Co}(\text{NO}_3)_2 \cdot 6\text{H}_2\text{O}$ (21.7 mg, 0.075 mmol) and Phen (24.8 mg, 0.125 mmol) in 4 mL of mixed solvents of DMF/DMA/ H_2O ($v/v/v = 1:1:2$) (DMF= Dimethyl Formamide and DMA= Dimethylacetamide) at 60 $^{\circ}\text{C}$ in a capped vial afforded orange crystals of **1** after two weeks, which were filtered, washed with H_2O , EtOH, Et_2O and dried at room temperature. (Yield: 75%, based on cobalt). Anal. Calc. (found) for $\text{C}_{51}\text{H}_{41}\text{N}_4\text{O}_{18}\text{Co}_2$: C, 54.90 (54.49); H, 3.70 (4.01); N, 5.02 (4.86) %. IR (KBr): $\nu(\text{cm}^{-1}) = 3350$ (m), 1617 (m), 1557 (s), 1423 (s), 1370 (s), 1275 (w), 1105 (w), 898 (w), 842 (m), 779 (m), 726 (s), 642 (m).

2.3. X-Ray Crystallography

A single crystal of the complex **1** with appropriate dimensions was chosen under an optical microscope and quickly coated with high vacuum grease (Dow Corning Corporation) before being mounted on a glass fiber for data collection. Data were collected on a Bruker Apex II Image Plate single-crystal diffractometer with a graphite-monochromated Cu $K\alpha$ radiation source ($\lambda = 1.54184 \text{ \AA}$) operating at 50 kV and 30 mA for complex **1**. All absorption corrections were applied using the multi-scan program SADABS [17]. In all cases, the highest possible space group was chosen. The structure was solved by direct methods using SHELXS-97 [18] and refined on F^2 by full-matrix least-squares procedures with SHELXL-97 [19]. Atoms were located from iterative examination of difference F-maps following least squares refinements of the earlier models. Hydrogen atoms were placed in calculated positions and included as riding atoms with isotropic displacement parameters 1.2 times U_{eq} of the attached C atoms. All structures were examined using the Addsym subroutine of PLATON [20] to ensure that no additional symmetry could be applied to the models. The crystallographic details of complex **1** are summarized in Table 1. Selected bond lengths and angles for complex **1** are collected in Table 2.

Table 1. Crystal data for complex 1.

Empirical Formula	$C_{23.5}H_{20.5}CoN_2O_9$
Formula weight	533.85
Temperature/K	294.49(10)
Crystal system	monoclinic
Space group	P_2/n
a/Å	7.7636(2)
b/Å	13.8680(4)
c/Å	21.1105(6)
$\alpha/^\circ$	90.00
$\beta/^\circ$	94.644(3)
$\gamma/^\circ$	90.00
Volume/Å ³	2265.42(11)
Z	4
ρ_{calc} mg/mm ³	1.565
m/mm ⁻¹	6.464
F(000)	1098.0
Index ranges	$-9 \leq h \leq 9, -16 \leq k \leq 14, -25 \leq l \leq 18$
Reflections collected	8335
Independent reflections	4036[R(int) = 0.0315]
Data/restraints/parameters	4036/0/331
Goodness-of-fit on F ²	1.053
Final R indexes [I >= 2 σ (I)]	R ₁ = 0.0503, wR ₂ = 0.1398
Final R indexes [all data]	R ₁ = 0.0667, wR ₂ = 0.1505
Largest diff. peak/hole/e Å ⁻³	1.31/−0.40

Table 2. Selected bond lengths (Å) and angles (°) for complex 1.

Co1-O1	2.066(2)	Co1-O2	2.138(2)	Co1-O3	2.103(3)
Co1-O6	2.127(3)	Co1-N14	2.118(3)	Co1-N15	2.141(3)
O1-Co1-O2	88.93(9)	O1-Co1-O3	89.25(11)	O1-Co1-O6	94.77(10)
O1-Co1-N14	92.63(10)	O1-Co1-N15	170.56(11)	O2-Co1-N15	91.35(10)
O3-Co1-O2	174.22(11)	O3-Co1-O6	86.05(12)	O3-Co1-N14	94.31(12)
O3-Co1-N15	91.35(11)	O6-Co1-O2	88.63(11)	O6-Co1-N15	94.67(11)
N14-Co1-O2	91.26(10)	N14-Co1-O6	172.60(11)	N14-Co1-N15	77.93(12)

3. Results and Discussion

3.1. Descriptions of the Crystal Structures

Complex 1 was prepared by a hydrothermal reaction of H₅DDCPBA, Co(NO₃)₂·6H₂O and Phen in mixed solvents of DMF/DMA/H₂O at 60 °C for two weeks and characterized by single-crystal X-ray crystallography, powder X-ray diffraction (PXRD), thermogravimetric analysis (TGA), and elemental analysis. Single-crystal X-ray analysis reveals that the photoresponsive molecular system is constructed by the connections of DDCPBA and Phen mixed ligands with a cobalt ion as node (Figure 1A). The Co(II) center has a distorted [CoN₂O₄] octahedral coordination sphere with two nitrogen atoms from one phen ligand, two oxygen atoms from two different DDCPBA ligands and two oxygen atoms from two different coordinated water molecules. The Co-N distances are 2.118(3) Å and 2.141(3) Å, the distances of Co-O_w are 2.103(3) Å and 2.127(3) Å, and Co-O distances are 2.066(2) Å and 2.138(2), respectively. It is worth pointing out that the coordination arrangements make the distances between the oxygen atoms of the carboxyl groups and the N atom of the phen ligand as follows: 3.0261(37), 3.0615(39), 3.0428(37) and 4.1927(37) Å, respectively. According to the previous reports [13,21], the distance (smaller than 3.7 Å) satisfies the requirements for an inter-ligand charge transfer. The carboxylate group in complex 1 adopts $\mu_1-\eta^1-\eta^0$ bridging modes to link two Co(II) ions

to form a 16-membered-ring (Figure 1B), and then the 16-membered-rings were connected to each other to furnish a 1D chain by the DDCPBA ligand (Figure 1C).

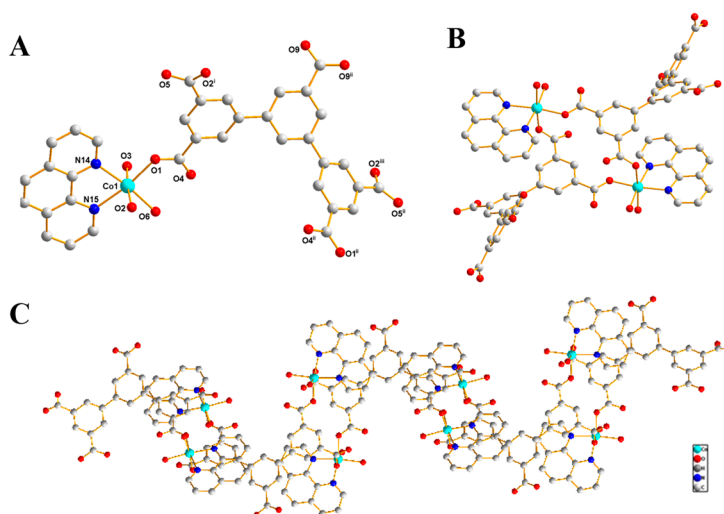


Figure 1. View of the coordination environment around Co(II) (A), the structure of the 16-membered ring (B) and the 1D chain (C) of **1** (Symmetry codes: (i) $1 - x, 1 - y, 1 - z$; (ii) $1.5 - x, y, 1.5 - z$; (iii) $0.5 + x, 1 - y, 0.5 + x$).

3.2. The Diffuse-Reflectance Spectra and ESR Spectra

The diffuse-reflectance spectra of the initial state and radical form of the complex **1** are shown in Figure 2. As shown in Figure 2, the diffuse-reflectance spectra of the orange crystal show absorption bands at 473 nm and 507 nm, which can be ascribed to the $\pi-\pi^*$ and $n-\pi^*$ transitions of the aromatic rings. However, upon UV irradiation (365 nm), the color of complex **1** changes to violet from orange, with new absorption bands appearing at about 572 nm and its intensity increases with extending the irradiation time. After about 1 h, the diffuse-reflectance spectra of complex **1** do not change any more. When complex **1** changed from orange to violet under UV irradiation, whether it be exposed to light irradiation or heating, the color of the sample will not change back. ESR measurement indicates that the coloration process is due to the generation of radicals ($g = 2.003$) (Figure 3), which is close to previous reports for free organic radicals [22].

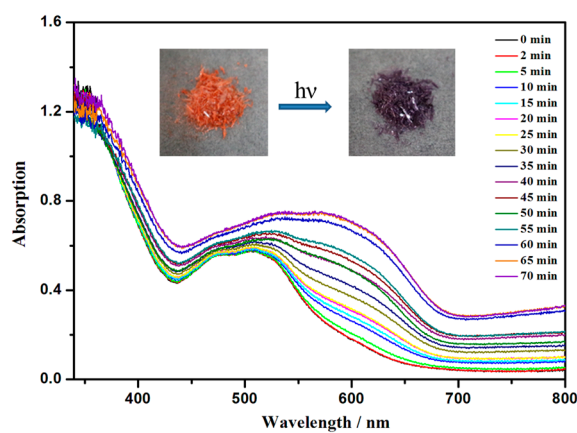


Figure 2. UV-vis diffuse-reflectance spectral changes of complex **1** upon Xenon lamp irradiation.

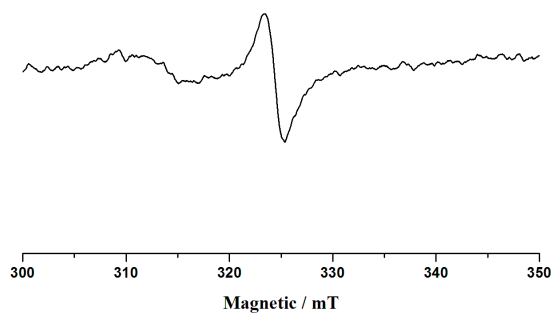


Figure 3. The ESR spectrum of the violet crystal **1**.

3.3. X-Ray Powder Diffraction Analysis

The phase purity of pink complex **1** is sustained by the powder X-ray diffraction pattern, Figure 4. Most of the peak positions of simulated and experimental patterns are in good agreement with each other; the differences in intensity may be due to the preferred orientation of the powder samples.

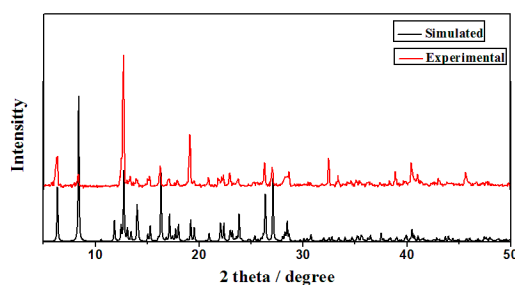


Figure 4. The powder XRD patterns and the simulated one from the single-crystal diffraction data for the complex **1**.

3.4. IR Spectra

The FT-IR spectrum of pink compound **1** was also investigated, Figure 5. The sharp bands at about 1557 cm^{-1} and 1423 cm^{-1} are attributed to asymmetric and symmetric stretching vibrations of the carboxylic group, respectively [22,23].

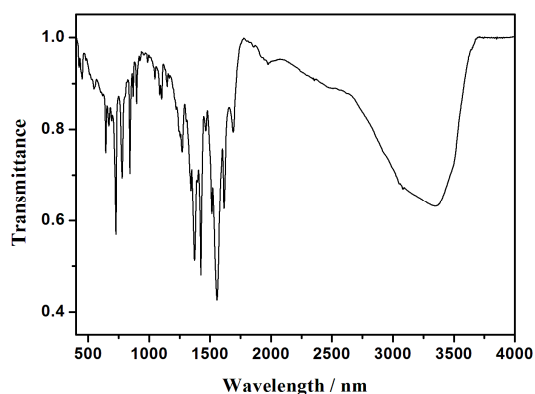


Figure 5. The IR (Infrared) spectra of the complex **1**.

3.5. Thermogravimetric Analyses

To assess the thermal stability and its structural variation with the temperature, thermogravimetric analysis (TGA) of orange complex **1** was performed under a N_2 atmosphere, Figure 6. Complex **1** has

two identifiable weight loss steps: The first one is consistent with the removal of two uncoordinated and two coordinated water molecules (obsd 14.53%, calcd 14.11%), which appears between 90 and 172 °C. The second one is attributed to the collapse of the framework, which is in the range of 345 to 445 °C. It is worth pointing out that the present complex **1** has better thermal stability than that of the pure organic photoresponsive materials, suggesting an effective way to develop photoresponsive materials based on metal–ligand complexes [24].

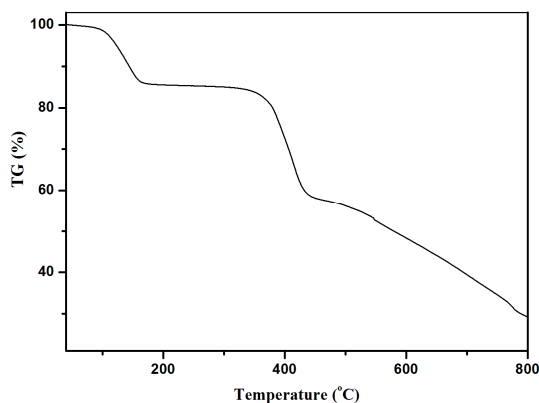


Figure 6. TGA curves for the complex **1**.

3.6. Magnetic Properties

The temperature dependence of magnetic susceptibilities for the orange complex **1** measured in the range of 2–300 K under the external magnetic field of 1000 Oe is shown in Figure 7. The $\chi_m T$ value at room temperature is $2.68 \text{ emu}\cdot\text{K}\cdot\text{mol}^{-1}$, which is higher than the spin only value of $1.875 \text{ emu}\cdot\text{K}\cdot\text{mol}^{-1}$ for the isolated high spin Co(II) ($S = 3/2$); this can be ascribed to the effects of the Spin-orbit coupling of the octahedral Co(II) ion [25] with the temperature decreasing; the $\chi_m T$ value remains almost constant from 300 to about 100 K. After this, the $\chi_m T$ value starts to decrease rapidly and reaches its lowest peak with the value of $1.55 \text{ emu}\cdot\text{K}\cdot\text{mol}^{-1}$ at 2 K. The magnetic susceptibility for the orange complex **1** conforms well to the Curie–Weiss law in a range of 2–300 K and gives the negative Weiss constant $\theta = -7.21 \text{ K}$ and the Curie constant $C = 2.78 \text{ emu}\cdot\text{K}\cdot\text{mol}^{-1}$.

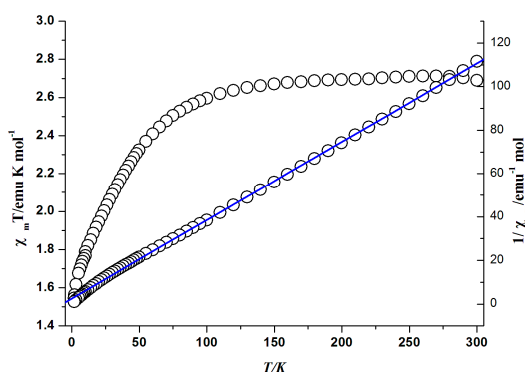


Figure 7. Temperature dependence of $\chi_m T$ for the complex **1**. The blue solid lines represent the best fitting in the temperature range of 2–300 K.

The field-dependent magnetizations measured up to 70 kOe at 2 K for complex **1**, as shown in Figure 8. The magnetization increases with a relatively fast speed with increasing field until 20 kOe, then increases smoothly up to about $2.6 \text{ M}/\text{em}\mu\cdot\text{g}^{-1}$ until 70 kOe. This data is only slightly lower than the saturated value of $3.0 \text{ M}/\text{em}\mu\cdot\text{g}^{-1}$ for an isolated Co(II) ion based on $g = 2.0$, indicating further that

there no obvious magnetic coupling exists between the Co(II) ions due to the long distance separated by the flexible organic ligands.

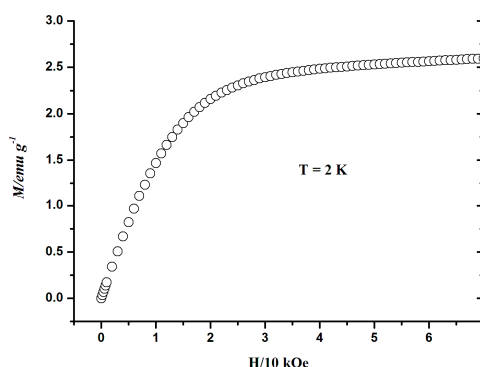


Figure 8. Plot of magnetization for the complex **1** at 2 K.

4. Conclusions

In conclusion, a novel photoactive system was constructed from two non-photoactive ligands and cobalt (II) ions. Upon UV irradiation (365 nm), orange crystal of **1** becomes violet. The ESR spectrum indicates that the photoactive phenomenon of complex **1** originates from an intermolecular energy transfer between the DDCPBA ligand and phenanthroline ligand.

Acknowledgments: We gratefully thank the financial support of the NSF of China (Grant No. 21301129), Shandong Provincial Natural Science Foundation (ZR2015BM005 and ZR2013BL016), and the China Postdoctoral Science Foundation (2015M572093). CCDC 1507467 contains the supplementary crystallographic data of complex **1** for this paper. These data could be obtained free of charge via www.ccdc.cam.ac.uk/conts/retrieving.html (or from the CCDC, 12 Union Road, Cambridge CB2 1EZ, UK; Fax: +44-1223-336033; E-mail: deposit@ccdc.cam.ac.uk).

Author Contributions: Jitao Lu and Qingguo Meng conceived and designed the experiments; Junhao Zhang and Rui Xun performed the experiments; Suqing Wang and Mingchao Chen analyzed the data; Jitao Lu wrote the paper.

Conflicts of Interest: The authors declare no conflict of interest.

References

- Sangeetha, N.M.; Maitra, U. Supramolecular gels: Functions and uses. *Chem. Soc. Rev.* **2005**, *34*, 821. [[CrossRef](#)] [[PubMed](#)]
- Li, C.P.; Du, M. Role of solvents in coordination supramolecular systems. *Chem. Commun.* **2011**, *47*, 5958. [[CrossRef](#)] [[PubMed](#)]
- Yin, Z.; Wang, Q.X.; Zeng, M.H. Iodine Release and Recovery, Influence of Polyiodide Anions on Electrical Conductivity and Nonlinear Optical Activity in an Interdigitated and Interpenetrated Bipillared-Bilayer Metal–Organic Framework. *J. Am. Chem. Soc.* **2012**, *134*, 4857–4863. [[CrossRef](#)] [[PubMed](#)]
- Chen, B.; Xiang, S.; Qian, G. Metal–Organic Frameworks with Functional Pores for Recognition of Small Molecules. *Acc. Chem. Res.* **2010**, *43*, 1115–1124. [[CrossRef](#)] [[PubMed](#)]
- O’Keeffe, M.; Yaghi, O.M. Deconstructing the Crystal Structures of Metal Organic Frameworks and Related Materials into Their Underlying Nets. *Chem. Rev.* **2012**, *112*, 675–702. [[CrossRef](#)] [[PubMed](#)]
- Talin, A.A.; Centrone, A.; Ford, A.C.; Foster, M.E.; Stavila, V.; Haney, P.; Kinney, R.A.; Szalai, V.; el Gabaly, F.; Yoon, H.P.; et al. Tunable Electrical Conductivity in Metal–Organic Framework Thin-Film Devices. *Science* **2014**, *343*, 66–69. [[CrossRef](#)] [[PubMed](#)]
- Zhou, X.P.; Liu, J.; Zhan, S.Z.; Yang, J.R.; Li, D.; Ng, K.M.; Sun, R.W.Y.; Che, C.M. A High-Symmetry Coordination Cage from 38- or 62-Component Self-Assembly. *J. Am. Chem. Soc.* **2012**, *134*, 8042–8045. [[CrossRef](#)] [[PubMed](#)]
- Zhao, X.L.; Liu, F.L.; Zhang, L.L.; Sun, D.; Wang, R.M.; Ju, Z.F.; Yuan, D.Q.; Sun, D.F. Achieving a Rare Breathing Behavior in a Polycatenated 2D to 3D Net through a Pillar-Ligand Extension Strategy. *Chem. Eur. J.* **2014**, *20*, 649–652. [[CrossRef](#)] [[PubMed](#)]

9. Peng, P.; Li, F.F.; Neti, V.; Metta-Magana, A.J.; Echegoyen, L. Design, Synthesis, and X-Ray Crystal Structure of a Fullerene-Linked Metal–Organic Framework. *Angew. Chem. Int. Ed.* **2014**, *53*, 160–163. [[CrossRef](#)] [[PubMed](#)]
10. Tai, X.; Wang, X.; You, H. Synthesis, Crystal Structure and Antitumor Activity of a New Zn(II) Complex Based on NAcetyl-L-phenylalanine and 1,10-Phenanthroline. *Chin. J. Struct. Chem.* **2016**, *35*, 586–590.
11. Zhang, L.; Kang, Z.; Xin, X.; Sun, D. Metal–organic frameworks based luminescent materials for nitroaromatics sensing. *CrystEngComm* **2016**, *18*, 193–206. [[CrossRef](#)]
12. Zeng, Y.; Fu, Z.; Chen, H.; Liu, C.; Liao, S.; Dai, J. Photo- and thermally induced coloration of a crystalline MOF accompanying electron transfer and long-lived charge separation in a stable host–guest system. *Chem. Commun.* **2012**, *48*, 8114–8116. [[CrossRef](#)] [[PubMed](#)]
13. Zeng, Y.; Liao, S.; Dai, J.; Fu, Z. Fluorescent and photochromic bifunctional molecular switch based on a stable crystalline metal–viologen complex. *Chem. Commun.* **2012**, *48*, 11641–11643. [[CrossRef](#)] [[PubMed](#)]
14. Chen, H.; Zheng, G.; Li, M.; Wang, Y.; Song, Y.; Han, C.; Dai, J.; Fu, Z. Photo- and thermo-activated electron transfer system based on a luminescent europium organic framework with spectral response from UV to visible range. *Chem. Commun.* **2014**, *50*, 13544–13546. [[CrossRef](#)] [[PubMed](#)]
15. Easun, T.L.; Jia, J.; Reade, T.J.; Sun, X.; Davies, S.E.; Blake, A.J.; George, M.W.; Champness, N.R. Modification of coordination networks through a photoinduced charge transfer process. *Chem. Sci.* **2014**, *5*, 539–544. [[CrossRef](#)]
16. Fu, Z.Y.; Chen, Y.; Zhang, J.; Liao, S.J. Correlation between the photoactive character and the structures of two novel metal organic frameworks. *J. Mater. Chem.* **2011**, *21*, 7895–7897. [[CrossRef](#)]
17. Bruker AXS Inc. *SMART, SAINT and SADABS*; Bruker AXS Inc.: Madison, WI, USA, 1998.
18. Sheldrick, G.M. *SHELXS-97, Program for X-ray Crystal Structure Determination*; University of Gottingen: Gottingen, Germany, 1997.
19. Sheldrick, G.M. *SHELXL-97, Program for X-ray Crystal Structure Refinement*; University of Gottingen: Gottingen, Germany, 1997.
20. Spek, A.L. *PLATON, A Multipurpose Crystallographic Tool*; Utrecht University: Utrecht, Netherlands, 2002.
21. Jhang, P.C.; Chuang, N.T.; Wang, S.L. Layered Zinc Phosphates with Photoluminescence and Photochromism: Chemistry in Deep Eutectic Solvents. *Angew. Chem. Int. Ed.* **2010**, *49*, 4200–4204. [[CrossRef](#)] [[PubMed](#)]
22. Xu, G.; Guo, G.C.; Guo, J.S.; Guo, S.P.; Jiang, X.M.; Yang, C.; Wang, M.S.; Zhang, Z.J. Photochromic inorganic–organic hybrid: A new approach for switchable photoluminescence in the solid state and partial photochromic phenomenon. *Dalton Trans.* **2010**, *39*, 8688–8692. [[CrossRef](#)] [[PubMed](#)]
23. Nakamoto, K. *Infrared and Raman Spectra of Inorganic and Coordination Compounds*; John Wiley & Sons: New York, NY, USA, 1986.
24. Zhang, L.; Guo, J.; Meng, Q.; Wang, R.; Sun, D. Syntheses, structures and characteristics of four metal–organic coordination polymers based on 5-hydroxyisophthalic acid and N-containing auxiliary ligands. *CrystEngComm* **2013**, *15*, 9578–9587. [[CrossRef](#)]
25. Rodríguez, A.; Kivekäs, R.; Colacio, E. Unique self-assembled 2D metal-tetrazolate networks: Crystal structure and magnetic properties of $[M(\text{pmtz})_2]$ ($M = \text{Co(II)}$ and Fe(II) ; Hpmtz = 5-(pyrimidyl)tetrazole). *Chem. Commun.* **2005**, *41*, 5228–5230. [[CrossRef](#)] [[PubMed](#)]

